NUMERICAL SOLUTION OF MODIFIED FOKKER-PLANCK EQUATION WITH POISSONIAN INPUT

Jiří Náprstek*, Radomil Král*

The paper makes a sketch of an SDOF system response analysis subjected to a random excitation having a form of the additive Poisson driven independent random impulses. A special generalised Fokker-Planck equation having a form of an integro-differential equation is presented together with boundary and initial conditions. Later the Galerkin-Petrov process as a method of a numerical solution of the respective evolutionary integro-differential equation for the probability density function (PDF) is presented in general. Various analytic and semi-analytic solution methods have been developed for various systems to obtain results requested. However numerical approaches offer a powerful alternative. In particular the Finite Element Method (FEM) seems to be very effective. Shape and weighting functions for purposes of a numerical solution procedure are carried out and corresponding ordinary differential system for PDF values in nodes is deduced. As a demonstration particular SDOF systems are investigated. Resulting PDFs are analysed and mutually compared.

Keywords: *Fokker-Planck equation, Poissonian excitation, numerical solution, transition effects*

1. Introduction

External loading affecting mechanical systems includes very often a significant random component. Papers are mostly oriented to random excitation of Gaussian white noises only. However, in practice a number of different excitation types emerge, which cannot be modeled in such a way even if various auxiliary filters are employed. The Poissonian chain of impulses is one of the most commonly known processes of this type.

Systems investigated are linear and non-linear. Despite the boundary is not very clear, it can be stated, that conventional methods being based on correlation and spectral approaches can be used for linear problems with additive Gaussian excitation only. Although also more complicated cases cannot be ruled out of their application, the utmost caution is necessary to keep a convergence to a meaningful result giving an answer corresponding with the original assignment. The Poissonian chain being a part of an excitation process either additive or multiplicative always implies a heavy complication. Spectral methods are excluded at all and moreover correlation processes in a classical meaning of the term are related to enormous difficulties. Their applicability is rather limited to linear systems only. Several attempts have been made to use a method of decomposition with respect to stochastic moments on the basis of initial differential system. Some instances can be found in the monograph [1]. Some more papers are worthy to be referenced, e.g. [2–3].

* Ing. J. Náprstek, DrSc., Ing. R. Král, Institute of Theoretical and Applied Mechanics ASCR, v.v.i., Prosecká 76, 190 00 Praha 9

Many uncertainties can be avoided using Markovian processes, unless the original differential system is investigated by means of the direct numerical integration. Their definition and subsequent application is a bit complicated, as Poissonian excitation part is discontinuous. For exclusively Gaussian excitation a special partial differential equation (PDE) for the unknown probability density function (PDF) can be inferred. This PDE is usually called Fokker-Planck (FP) equation. Analogously for combined excitation (Gauss-Poisson) a similar PDE being called generalized Fokker-Planck (GFP) can be derived as well. Also other names are in use.

The GFP equation has an integro-differential character and moreover similarly like the FP has an evolutionary character. Consequently, the GFP is able to describe any transition process running starting initial conditions as far as the steady state if it exists. If the relevant solution succeeds to be found, it can be taken as a natural extension of a deterministic result. It gives the full information about a response random character and enables to deduce also additional special attributes of the response, such as frequency structure, local stability, etc.

2. Generalized Fokker-Planck equation

A response of the mechanical system results from an external excitation. Basically they are of deterministic and random character. Authors recently have been dealing with FP equation under exclusively Gaussian excitation, see e.g. [4]. Let us extend the initial differential system by an influence of the Poissonian random chains. Thus the excitation random part consists now of Gaussian and Poissonian parts. Influence of both random excitation parts will be introduced as independent. Everyone is included in a form of linear combinations of individual state variables or their functions. The initial differential system can be expressed with a sufficient generality as follows:

$$\frac{\mathrm{d}x_j(t)}{\mathrm{d}t} = f_j(\mathbf{x},t) + g_{jr}(\mathbf{x},t)\, w_r(t) + c_j \cdot Y(t)\ , \quad \mathbf{x} = [x_1,\ldots,x_n] \tag{1}$$

$Y(t)$ – Poissonoian chain following the definition: $Y(t) = \sum_{i=1}^{N(t)} Z_i \cdot \delta(t - t_i)$,

Z_i – sequence of random impulses; impulses are considered 'rectangular' with a constant width and random amplitude; their position on the time coordinate corresponds with Poissonian distribution with the characteristic value λ.

$p_z(\zeta)$ – probability density of impulse amplitudes Z_i.

c_i – constant parameters specifying an influence of the chain $Y(t)$ in individual equations (1); the chain $Y(t)$ applies in the system (1) as an additive noise only without any possibility of a deterministic modulation.

$w_r(t)$ – Gaussian continuous white noises with a constant cross-density in a meaning of stochastic moments: $K_{rs} = \mathbf{E}\{w_r \cdot w_s\};\ r,s = 1,m.$

$f_j(\mathbf{x},t)$, $g_{jr}(\mathbf{x},t)$ – continuous deterministic functions of state variables and time $j = 1,n$; noises can act as additive as well as multiplicative with possible deterministic modulation.

In principal even more general formulation of the system (1) are possible. The components of the random excitation can be considered inside of one non-linear functional prescription on a right side of the respective equation. Nevertheless such cases are very

seldom to see. Even mathematical literature devote oneself to those only rarely. Indeed, even non-linear input of random processes can be mostly handled extending the original system in such a way that finally the type of system (1) with a linear input of both types of random processes is regained. The general formulation would claim a more complicated mathematical background. Anyway, the contribution for tasks of theoretical mechanics and physics would be very small in comparison with the linear formulation. However special cases exist being treated using dedicated procedures.

The GFP equation for the unknown PDF of the response in variables $\mathbf{x}, t$ can be assigned to the system (1). The FP equation (without Poissonian chains) together with detailed derivation and analysis of various attributes can be found in a number of monographs, see for instance [2], [5–6] and many others. The GFP completed by an influence of Poissonian chains is devoted in [6] for constant as well as randomly variable impulse amplitudes including special cases. On the theory of general processes affecting on the input of stochastic differential systems dwells the monograph [7]. All subsequent papers dealing with Poissonian processes are referencing this one. The respective GFP equation corresponding with the system (1) can be written with respect to [8–9] in the form:

$$\frac{\partial p(\mathbf{x},t)}{\partial t} = -\frac{\partial}{\partial x_j}\left(\kappa_j(\mathbf{x},t)\cdot p(\mathbf{x},t)\right) + \frac{1}{2}\,\frac{\partial^2}{\partial x_j\,\partial x_k}(\kappa_{jk}(\mathbf{x},t)\cdot p(\mathbf{x},t)) - \\ - \lambda p(\mathbf{x},t) + \lambda \int_{-\infty}^{\infty} p(\mathbf{x}-\mathbf{c}\cdot\zeta,t)\,p_z(\zeta)\,\mathrm{d}\zeta\ , \tag{2}$$

$$\begin{aligned} &\text{drift coefficients:} && \kappa_j(\mathbf{x},t) = f_j(\mathbf{x},t) + \frac{1}{2}\,K_{rs}\cdot g_{ls}(\mathbf{x},t)\,\frac{\partial g_{jr}(\mathbf{x},t)}{\partial x_l}\ , \\ &\text{difusion coefficients:} && \kappa_{jk}(\mathbf{x},t) = K_{rs}\cdot g_{jr}(\mathbf{x},t)\,g_{ks}(\mathbf{x},t)\ . \end{aligned} \tag{3}$$

There is a question what solution method of the GFP in case of a specific mechanical system should be selected. Unlike the Gaussian excitation the literature concerning the Poissonian excitation is not by far so rich. Also special cases which allow to be solved analytically either in closed or approximative form are very rare. Apart from cited monographs [1], [6] and primarily [7] a few papers exist devoted to various semi-analytic approximative procedures. Their structure usually corresponds with a character of a result which is pursued. Let us quote papers [9–16], or possibly one chapter in the monograph [1]. However these studies are rather dealing with basic analytic problems of Poissonian processes implementation into systems of the type (1). Moreover their conclusions are not in a full agreement.

Among semi-analytic techniques striving for a solution of a non-steady problem of Eq. (2) some procedures being based on eigen-functions and eigen-values of the FP operator should be mentioned, see e.g. [10]. Several asymptotic method have been applied especially in the domain of first excursion problem, see monograph [18].

Anyway a very powerful tool for the FP and GFP equations reveal to be numerical methods. On the basis of their own research and of other references authors showed in [4] the compass of the FEM application solving the FP equation. Despite the purely numerical solutions inevitably suffer from many shortcomings, several important PDF features non-identified by other methods succeeded to be found.

The comprehensive overview regarding the application of numerical methods for the FP equation analysis including also the GFP equation has been published in 1997, see [19].

Before and after this date a number of papers have appeared dealing with FEM applications on the FP equations. The first attempts at the FEM applications on the FP equation analysis get to seventieth. Let us mention for instance [20–24], etc. Despite their contribution is indisputable, the number of authors getting on is still rather limited.

The GFP operator is not self-adjoint. In order to overcome this and other obstacles the variational methods being based on orthogonalization principles should be employed. Thus as a basis of further analysis the Galerkin-Petrov method has been selected. Various aspects of special variants of the FEM related with the Galerkin method adaptation and implementation for the FP equation have been studied by many authors. Problems of steady-state solutions are widely studied for instance in [25–26], multiscale implementation among others [27], etc.

The efficiency of the FEM in the FP equation analysis seems to be large. It applies particularly to some detailed features of the PDF in transition phases where the FEM is hardly replaceable, see e.g. [28]. To formulate a solution when some state variables can gain values only within a given limited interval and being subdued to more complicated boundary conditions doesn't represent difficulties. The tool of FE enables to abandon an assumption of Gaussian inputs to system (1) without serious troubles, which is very complicated when using other approaches. Provided that the FP equation succeeds to compose even for other input noises, e.g. Poissonian chains, the method is working quite reliably, see for instance [11] with the link to additional papers, e.g. [12–13], [17].

The literature appraisal proved, that unlike the FP the direct FEM solution of the GFP equation probably nobody attempted until now. A certain complication when including the Poissonian excitation represents the convolution in the second part of the GFP equation (2). Sometimes authors eliminate this one using Fourier transform in coordinates where Poissonian excitation is employed, see e.g. [8]. This step results in the system of ordinary differential equations, which is subsequently solved by means of the network method. The solution is obtained in a form of the Fourier transform, which reveals to be a significant disadvantage of this procedure. Provided the result is not satisfactorily described by the characteristic function of the PDF, then the inverse Fourier transform should be done indispensably.

Let us take that the missing Gaussian part of excitation leads to significant simplification of Eq. (2), as the diffusion terms ($\kappa_{jk} = 0$) vanish, see e.g. [16]. In case that amplitudes of Poissonian impulses get to be constant (time sequence only remains random), the density $p_z(\zeta)$ reduces to the Dirac function with non-zero value in point ζ_0. The respective convolution degenerates to an ordinary member with a shifted argument $\lambda \cdot p(\mathbf{x} - \mathbf{c} \cdot \zeta_0)$.

Let us remember some shortcomings of the FEM in this application. To introduce a genuine deterministic initial condition for PDF in a form of the Dirac function is hardly possible. However it doesn't matter so far. Some worse is a problem with rising number of independent variables with increasing degrees of freedom of the system (1). Anyway also analytic methods suffer from this fact. Here proves this pitfall by a necessity to evaluate the integrals over finite elements in a space with high number of dimensions (n degrees of freedom represents $2\,n$ space dimensions). An extent of the ordinary differential system which emerges discretizing the expression on the right side of Eq. (2) growth exponentially. A bit problematic can become the solution of the steady-state problem (zero left side of Eq. (2)) notably at the infinite multidimensional domain.

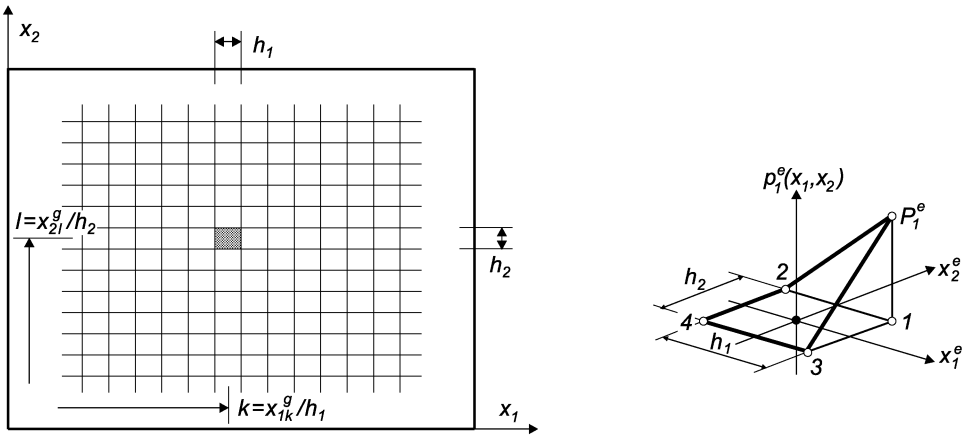

Fig.1: Domain splitting into finite elements with respect to displacement x_1 and velocity x_2; outline of the PDF approximation within one finite element

For all it seems that strengths probably prevail weaknesses in many important cases and the FEM could be able to provide an important effective tool of the FP equation analysis. In following sections several demonstrating examples of SDOF systems with an additive Poissonian excitation will be presented. However, before that several special properties of finite elements and methods of numerical integration used should be noticed.

The GFP equation is linear and in individual cases they will be discussed (SDOF systems) only in two phase coordinates x_1, x_2 (displacement, velocity) and with an additive excitation. Therefore the problem of a significant multi-dimensionality of elements falls away and conventional methods of integration can be used. Taking into account that the GFP is of the second order in space coordinates, elements with linear approximation between nodes are sufficient. In order to avoid any secondary inhomogeneity the domain has been split up into rectangular elements of identical size without any adaptations of more 'dramatic' PDF changes.

Following nomenclature has been introduced in accordance with Fig. 1 :

x_1^e, x_2^e – local coordinates within one finite element with respect to its center,

x_1, x_2 – global coordinates,

x_{1k}, x_{2l} – global coordinates of the element center (k, l),

$p_i^e(x_1^e, x_2^e)$ – shape functions; $i = 1, 4$,

P_i^e – PDF values in element nodes; subscript has a local meaning; $i = 1, 4$,

h_1, h_2 – finite element dimensions.

where it holds:

$$x_1 = x_{1k}^g + x_1^e \ , \qquad x_2 = x_{2l}^g + x_2^e \ . \tag{4}$$

Functions g_{jr}, see Eqs (1), (3) became constants as follows: $g_{11} = g_1 = 0$, $g_{21} = g_2 = 1$. Let us accept an assumption that the Poissonian excitation will be applied in coordinate x_2 only. Thus a model of an SDOF system excited by random impulses is prepared.

The operator of Eq. (2) is of the second order. In order to warrant a convergence in the mean when using a procedure of Galerkin type the linear approximation is satisfactory. Respecting conventions as mentioned one can introduce within a domain of the rectangular

finite element usual approximation functions in a following form, see Fig. 1 :

$$p^e(x_1^e, x_2^e) = \sum_{i=1}^{4} P_i^e \cdot p_i^e(x_1^e, x_2^e) \ , \qquad p_i^e(x_1^e, x_2^e) = p_i^e \ ,$$

$$p_1^e = \frac{(h_1 + 2\,x_1^e)\,(h_2 + 2\,x_2^e)}{4\,h_1\,h_2} \ , \qquad p_2^e = \frac{(h_1 - 2\,x_1^e)\,(h_2 + 2\,x_2^e)}{4\,h_1\,h_2} \ , \tag{5}$$

$$p_3^e = \frac{(h_1 + 2\,x_1^e)\,(h_2 - 2\,x_2^e)}{4\,h_1\,h_2} \ , \qquad p_4^e = \frac{(h_1 - 2\,x_1^e)\,(h_2 - 2\,x_2^e)}{4\,h_1\,h_2} \ .$$

Further adaptations in the meaning of the Galerkin-Petrov method should be applied primarily to the differential part (left side and then the first, second and third member on the right side of Eq. (2), see e.g. [4]. To introduce the approximation (5) into Eq. (2) means in compliance with known algorithms to replace the sought-after function $p(x_1, x_2, t)$ in the whole definition area by a complicated broken function. It employs in a domain of a particular element by force the product of the approximation (5) and an expression composed of Heaviside functions ('unit window'). This function attains one inside of this element and zero elsewhere. Consequently, after substitution of approximation (5) into Eq. (2) the next step consists in an individual multiplication by every of four shape functions including the relevant 'unit window' and in an integration over the whole domain. The unit window brings about that the integration provides non-zero results only within limits of the respective element. Individual terms of the Eq. (2) give matrices (4×4) in local coordinates. Thus matrices $\mathbf{M}^e$, $\mathbf{S}^e$ (4×4) are obtained for one finite element (k, l). Individual matrix elements can be evaluated using formulae:

$$M_{ij}^e = \int_\Omega p_i^e(x_1^e, x_2^e)\, p_j^e(x_1^e, x_2^e)\, \mathrm{d}x_1^e\, \mathrm{d}x_2^e \ , \qquad \Omega \text{ – integration domain of one element} \ , \tag{6}$$

$$\begin{aligned} S_{ij}^e = \int_\Omega \Bigg[& p_i^e(x_1^e, x_2^e)\, p_j^e(x_1^e, x_2^e) \left(\frac{\partial f_1(x_1, x_2, t)}{\partial x_1} + \frac{\partial f_2(x_1, x_2, t)}{\partial x_2} \right) + \\ & + p_i^e(x_1^e, x_2^e) \left(f_1(x_1, x_2, t)\, \frac{\partial p_j^e(x_1^e, x_2^e)}{\partial x_1^e} + f_2(x_1, x_2, t)\, \frac{\partial p_j^e(x_1^e, x_2^e)}{\partial x_2^e} \right) + \\ & + K_{aa} \frac{\partial p_i^e(x_1^e, x_2^e)}{\partial x_2^e} \frac{\partial p_j^e(x_1^e, x_2^e)}{\partial x_2^e} \Bigg] \mathrm{d}x_1^e\, \mathrm{d}x_2^e \ . \end{aligned} \tag{7}$$

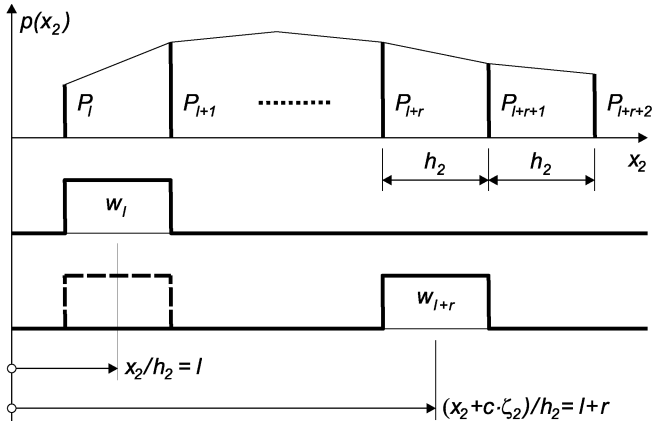

Fig.2: Argument shift

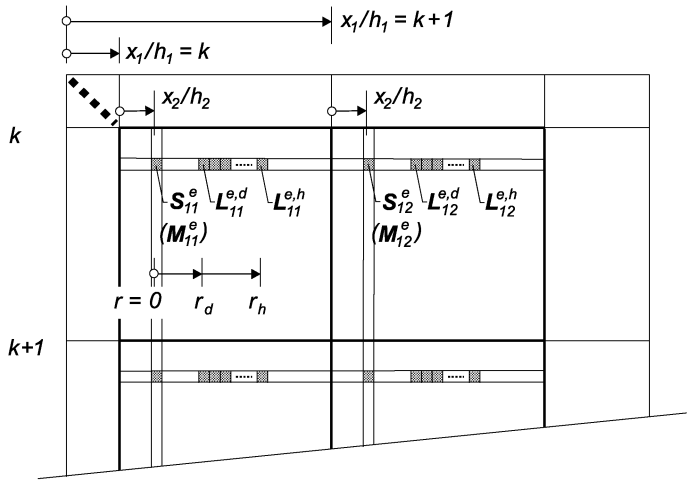

Fig.3: Outline of local matrices emplacement into global ones

To evaluate the integration in (7) it is necessary to respect that f_1, f_2 are functions of global coordinates corresponding to (4). These functions are approximated in the framework of one element either by function values in point (x^g_{1k}, x^g_{2l}), or more precisely by a linear functions in a proximity of these function values. The matrix $\mathbf{S}^e$ includes an influence of the first two terms on the right side in Eq. (2).

The next step consisting in deposition to the global matrices is apparent due to the network in use. The transformation to global coordinates in this case is very easy. For every finite element local matrices $\mathbf{M}^e$, $\mathbf{S}^e$ accordingly to Eqs (6), (7) are modified with respect to position (x^g_{1k}, x^g_{2l}) of the particular element and then they are added onto corresponding places of global matrices $\mathbf{M}$, $\mathbf{S}$, see Figs 2, 3. The scheme in Fig. 3 corresponds to nodes numbering following x_2, or l and in upper level cycle following x_1, or k respectively. Submatrices $\mathbf{M}^e_{11}$, $\mathbf{M}^e_{12}$, etc. are of the type 2×2 and they represent the mean upper-left or upper right quarter of the original matrix $\mathbf{M}^e$. If the general numbering is used, then depositing into global matrices should be done individually taking separately each of 16 elements of matrices $\mathbf{M}^e$, $\mathbf{S}^e$.

Thus all finite elements should be processed. Finally we obtain the system of ordinary differential equations for unknowns $\mathbf{P}(t)$ being functions of time. This procedure has been used for exclusively Gaussian excitation in the paper [4]. In general it is widely known and for operators without argument shifting is worked out very precisely.

Let us take the convolution part in Eq. (2). Let us suppose that $p_z(\zeta)$ is non-zero only within the interval $\zeta \in (\zeta_d - h_2/(2c), \zeta_h + h_2/(2c))$, whereas the interval limits ζ_d, ζ_h are integer multiples of h_2/c. The given PDF $p_z(\zeta)$ should be distributed along the axis x_2 into sections coinciding with the division into finite elements along the axis x_2. It means that the global coordinate ζ is described within one finite element by the transforming expression:

$$\zeta = \zeta^g_r + \zeta^e \ , \qquad \zeta^e \in \left(-\frac{h_2}{2\,c}, \frac{h_2}{2\,c} \right) \tag{8}$$

where $c \cdot \zeta^g_r$ denotes the coordinate of the center and $c \cdot \zeta^e$ the local coordinate inside the element. The subscript r of this element implies the shift to right from the initial position l to the resulting value $l + r$.

Let us admit for a while that $p_z(\zeta)$ is non-zero only within one finite element r getting constant value p_{zr}. Under these conditions the integral in Eq. (2) vanishes and it is substituted by a multiplication of the integrand by value $p_{zr} \cdot h_2/c$. In Eq. (2) the unknown with a shifted argument $x_2 - c \cdot \zeta_r^g$ appears. Therefore the 'unit window' positioned in point x_{2l} (intended to multiply Eq. (2)) matches with the unknown approximated accordingly with Eq. (5) only when the x_2 shifts by $c \cdot \zeta_r^g$. Result of the integration over one finite element doesn't change as in the integrand no coefficients f_1, f_2 are presented, however the unknowns superscript l increases accordingly along x_2 by value $r = c \cdot \zeta_l^g / h_2$. It implies that the local matrix $\mathbf{L}^{er}$ (corresponding to the matrix $\mathbf{M}^e$, see Eq. (6)) should be multiplied by $\lambda \cdot h_2$ and deposited by r places right from the main diagonal of the global matrix $\mathbf{S}$. It represents one finite element and an impulse loading the amplitude of which is given by the uniform distribution (except the multiplier c) within one finite element.

Provided that $p_z(\zeta)$ is positive on an interval larger than one finite element, the procedure should be repeated, but the shift from the main diagonal has to be modified accordingly. The shifting index rises within the interval $r = c \cdot \zeta_d/h_2,\ c \cdot \zeta_h/h_2$. The whole algorithm is outlined in Figs 2 and 3. So the complementing matrix $\mathbf{L}$ can be expressed as follows:

$$\mathbf{L} = \sum_{r=c\cdot\zeta_d/h_2}^{c\cdot\zeta_h/h_2} \mathbf{L}^r \tag{9}$$

where $\mathbf{L}^r$ corresponds to the global matrix complement for the r-th part of $p_z(\zeta)$ including the relevant emplacement, or in other words including the transformation into global coordinates and deposition to the global matrix after multiplication by coefficients λ, h_2. Consequently, summation in Eq. (9) has rather a symbolic meaning.

The system of ordinary differential equations for PDF values in the mesh nodes can be expressed in a symbolic way:

$$\mathbf{M}\,\frac{\mathrm{d}\mathbf{P}}{\mathrm{d}t} = (\mathbf{S} - \lambda\,\mathbf{M} + \lambda \cdot h_2\,\mathbf{L})\mathbf{P} \tag{10}$$

where $\mathbf{P}$ is a vector of unknown values PDF.

As the method of numerical integration of the system of ordinary differential equations (10) proved the best the procedure of predictor-corrector type based on the Adams algorithm, see e.g. [28].

3. Linear system with additive Poissonian excitation

Let us pay attention to a single degree of freedom (SDOF) system with a random excitation of Poissonian type:

$$\begin{aligned} \ddot{x} + 2\,\omega_b\,\dot{x} + \omega_0^2 \cdot x = c \cdot Y(t) \quad \Rightarrow \quad & \dot{x_1} = x_2\ , \\ & \dot{x_2} = -\omega_0^2\,x_1 - 2\,\omega_b\,x_2 + c \cdot Y(t)\ . \end{aligned} \tag{11}$$

The process $Y(t)$ is a stationary Poissonian chain, where it has been put $c_1 = 0$, $c_2 = c$. Diffusion coefficients are vanishing, because in Eq. (7) no Gaussian excitation processes are employed. For this reason the member with second derivatives in Eq. (2) disappears. Drift coefficients follow immediately from formulae (3):

$$\kappa_1 = x_2\ , \qquad \kappa_2 = -\omega_0^2\,x_1 - 2\,\omega_b\,x_2\ . \tag{12}$$

Introducing Eq. (12) into Eq. (2) the relevant FP equation can be obtained from its general form after an adequate modification:

$$\frac{\partial p(x_1,x_2,t)}{\partial t} = -\frac{\partial[x_2\,p(x_1,x_2,t)]}{\partial x_1} + \frac{\partial[(\omega_0^2\,x_1 + 2\,\omega_b\,x_2)\,p(x_1,x_2,t)]}{\partial x_2} - \\ - \lambda\,p(x_1,x_2,t) + \lambda \int_{-\infty}^{\infty} p(x_1,x_2 - c\cdot\zeta,t)\,p_z(\zeta)\,\mathrm{d}\zeta \tag{13}$$

Probability density $p_z(\zeta)$ is assumed to be constant with an amplitude q within the interval $\zeta \in (D_1, D_2)$, where $D_1 = \zeta_d - h_2/(2c)$, $D_2 = \zeta_h + h_2/(2c)$, as it coincides with an explanation in the previous part. Therefore impulses are altogether positive and each of them containes a finite energy.

The unknown $p(x_1, x_2, t)$ should be approximated in compliance with (5). The further procedure follows Galerkin-Petrov method. The result of integration for one finite element of the domain is a system of four ordinary differential equations of the first order.

For the numerical solution of Eq. (9) following parameter values have been selected: $\omega_0^2 = 1.0$, $\omega_b = 0.1$, $K_{aa} = 0.0$, $K_{ab} = K_{bb} = 0.0$. The excitation is started in the point $t = 0$. We suppose that the system is in a standstill in this moment.

The initial condition for the PDF is selected in a form:

$$p(x_1,x_2,0) = N\cdot\exp\left(-\frac{\omega_0^2\,(x_1 - x_{1,0})^2}{\sigma^2}\right)\,\exp\left(-\frac{(x_2 - x_{2,0})^2}{\sigma^2}\right) \tag{14}$$

where $N = 1/2\,\pi\,\sigma^2$, $\sigma^2 = 1/9$. For a small value σ^2 the initial condition (14) approaches to the Dirac function requested earlier. The approximation (14) admits that the movement of the system (11) doesn't start with certainty in the point ($x_{1,0}$, $x_{2,0}$ as it would correspond to the Dirac function, but a small scatter of the response initial state in the neighborhood of this point is allowed. The apex of the function (14) will be emplaced for the linear system to the origin ($x_{1,0} = 0$, $x_{2,0} = 0$).

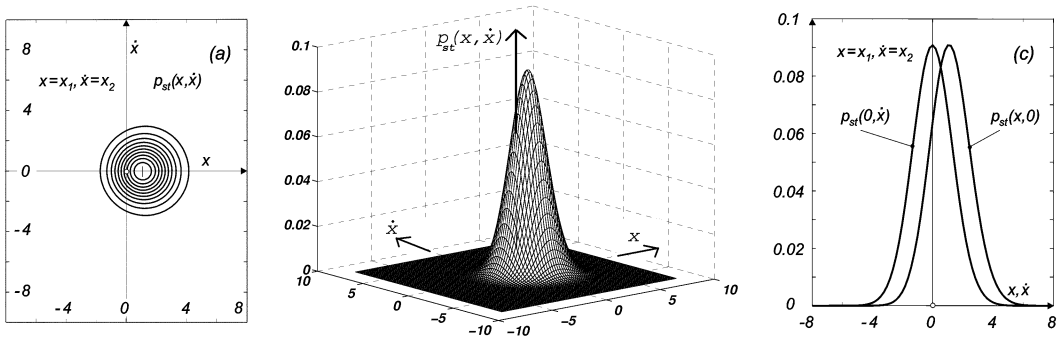

Fig.4: Response PDF of a linear system with an additive Poissonian excitation; (a) contour diagram; (b) axonometric view; (c) vertical sections in the surface apex following axes $x, \dot{x}$

Assembling partial approximations mentioned above the differential system of the type (10) can be composed. The integration domain size should be adequately large, similarly like in [4], in order that the $p(x_1, x_2, t)$ value on its boundary can be put zero. Thus

the value $p(x_1, x_2, t) = 0$ on the domain boundary can be used as the boundary condition for every t. When loading local matrices $\mathbf{L}^e$ into the global matrix, see Eq. (10), some elements fall outside defined field of the global matrix in its peripheral parts. Influence of these elements is neglected. In order to be entitled to accept this approach, the meshing has to be satisfactorily fine and boundaries far away places of important PDF changes. These parameters cannot be determined exactly. The task should be evaluated several times inserting small variations into the boundary position and the nodes distribution with respect to oscillator parameters and an interval of Poissonian excitation.

As a testing example a classical linear system following Eq. (1) with parameters $\omega_0^2 = 1.0$, $\omega_b = 0.1$ together with excitation parameter $c = 1$ has been selected. Intensity of the Poissonian chain varies within the interval $\lambda = 1.0, \ldots, 10.0$. The amplitude complies with the element where the positive probability of acting impulses occurs. These zones are adopted either successively for individual ζ_r^g corresponding with $r = 2, \ldots, 9$, or accumulatively like broader intervals $r = 1 \div 2, r = 1 \div 3, \ldots, r = 1 \div 7$. The integration domain of Eq. (13) is introduced as follows: $x = x_1 \in (-20, 20)$, $\dot{x} = x_2 \in (-20, 20)$; the domain is divided in every direction into 200 elements, e.g. $h_1 = 0.2$, $h_2 = 0.2$.

The general overview of the PDF character concerning the steady-state after transition effect disappears can be made observing Fig. 4, see $p_{st}(x, \dot{x})$. Response mathematical mean shifted from the origin (initial condition) along the x, or x_1. It reached this point following a sharp spiral. Position of the mathematical mean indicates, that the displacement will be positive and the velocity vanishing with a high probability. The contour diagram shows a modest skewness towards the origin. The axonometric view and vertical sections demonstrate that the PDF in both coordinates resembles the Gaussian character despite the third and fourth moments are getting to move away a bit.

Results of more detailed investigation of the response PDF character concerning the above SDOF system are demonstrated in Figs 5–7. The layout of these pictures is analogous. Part (a) represents the vertical section of the PDF in a steady-state along the axis x-displacement, denoted $p_{st}(x, 0)$. Everyone of these sections is normalized. In part (b) under identical conditions the vertical sections following the axis $\dot{x}$-velocity are plotted, denoted $p_{st}(0, \dot{x})$. Horizontal scales in all parts (a) are identical, the same is valid concerning parts (b).

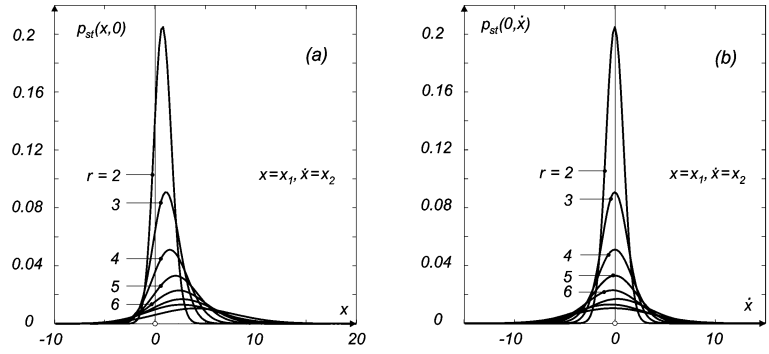

Fig.5: Response PDF of a linear system under excitation in a domain of elements ζ_r^g, $r = 2, 3, \ldots, 9$; density $\lambda = 2.0$; $\omega_0 = 1.0$, $\omega_b = 0.1$; (a) vertical sections along axis $x = x_1$-displacement; (b) vertical sections passing the surface apex along axis $\dot{x} = x_2$-velocity

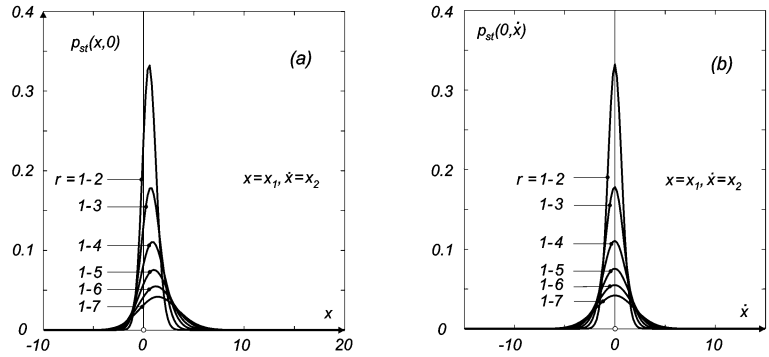

Fig.6: Response PDF of a linear system under excitation in a domain of elements ζ_r^g, $r = 1 \div 2, r = 1 \div 3, \ldots, r = 1 \div 7$; density $\lambda = 2.0$; $\omega_0 = 1.0$, $\omega_b = 0.1$; (a) vertical sections along axis $x = x_1$-displacement; (b) vertical sections passing the surface apex along axis $\dot{x} = x_2$-velocity

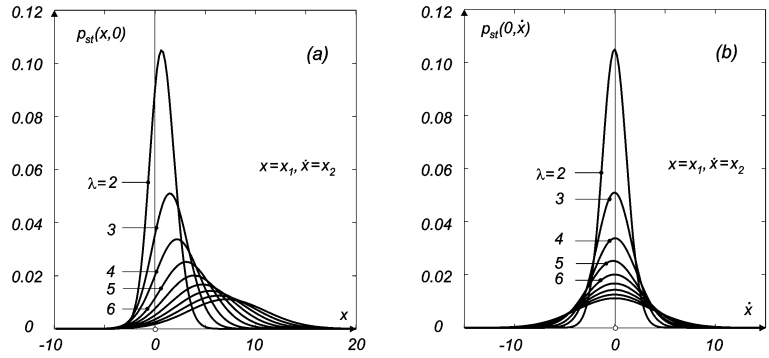

Fig.7: Response PDF of the linear system under excitations with densities $\lambda = 2, 3, \ldots, 10$; area of the element ζ_r^g, $r = 4$; $\omega_0 = 1.0$, $\omega_b = 0.1$; (a) vertical sections along axis $x = x_1$-displacement; (b) vertical sections passing the surface apex along axis $\dot{x} = x_2$-velocity

Vertical sections regarding zones $r = 2, \ldots, 9$ are depicted in Fig. 5. They reflect conditions when impulse amplitudes vary only in a very small range of one finite element and therefore they can be taken as constant. Therefore the intensity of an adequate Poissonian excitation process is adopted as constant value $\lambda = 2.0$. The part (a) makes obvious that the response mathematical mean rises with increasing r. Maximum of the PDF drops while response variance increases. The skewness of the $p_{st}(x, 0)$ is mildly positive, nevertheless it doesn't disturb the symmetry of the curve too much with respect to the mathematical mean. Anyway this tendency is a follow-up to the initial condition (14). The velocity PDF is symmetric in this series having a zero mathematical mean. Its maximum drops and variance rises.

A similar trend can be observed in the Fig. 6. The PDF section series corresponds to excitation given by impulses with amplitudes driven by a uniform distribution in area $r = 1$ and 2, later in area $r = 1 \div 3$ until area $r = 1 \div 7$. The impulse amplitude density is in the last case positive and constant in the interval $r = 1, \ldots, 7$ and vanishing elsewhere. Absolute values of system response are in such a case significantly larger in comparison with

λ (1)	M_1 (2)	M_{2c} (3)	M_{3c} (4)	M_{3c}^G (5)	M_{4c} (6)	M_{4c}^G (7)
2.0	0.764	1.159	0.318	0.0	8.017	7.544
3.0	1.580	3.221	0.650	0.0	31.898	31.130
4.0	2.285	4.847	0.977	0.0	71.670	70.490
5.0	3.199	6.474	1.300	0.0	127.340	125.750
6.0	3.982	8.120	1.628	0.0	200.000	197.820
7.0	4.798	9.752	1.948	0.0	287.580	285.340
8.0	5.607	11.381	2.226	0.0	390.490	388.570

Tab.1: Stochastic moments of the displacement in a steady-state for the increasing λ, $r = 4$

individual r. It is obvious from the grafical demonstration in the figure (a), that the response mathematical mean shifts higher in comparison with Fig. 5(a). The quantitative difference in displacement amplitudes is not visible too much as all PDF curves are normalized.

Influence of the rising density λ of the exciting Poissonian process is depicted out in Fig. 7. The PDF evolution of the displacement for values $\lambda = 2, \ldots, 10$ and constant value $r = 4$ is demonstrated in part (a), concerning velocity in part (b). The rising density has an evident influence on the mathematical mean value increase, local PDF maximum diminishing and variance growth. Selected results of numerical evaluation are also given in Tab. 1. For rising λ there are taken out first four moments enabling a rough comparison with an influence of a common Gaussian process :

M_1 – mathematical mean value, or the most probable displacement of the system discussed in a steady-state;

M_{2c} – central second moment, or displacement variance;

M_{3c} – third central moment, or displacement skewness;

$M_{3c}^G = 0.0$ – displacement skewness due to Gaussian excitation;

M_{4c} – fourth central moment, or displacement sharpness;

$M_{4c}^G = 3 * M_{2c}^2$ – displacement sharpness due to Gaussian excitation.

It follows out of the second column of Tab. 1 and of Fig. 7(a) how a certain 'effective' displacement is rising with rising intensity of the excitation process. Interpretation of the displacement variance in the third column is obvious. The fourth (skewness) and sixth (sharpness) columns can be used to indicate the difference from results due to Gaussian excitation. A skewness of the Gaussian process vanishes as we can see in the fifth column. The actual skewness in the fourth column is non-negligible. Let us assess the sharpness. If the process is Gaussian, then the sharpness should provide values following the seventh column. However values in the sixth and seventh columns differ. Despite that we can conclude that the result doesn't differ significantly from the Gaussian process. Hence an important implication of the central theorem is validated and in particular that the non-Gaussian process being filtered throughout the linear system with constant coefficients approaches to Gaussian process.

If some rough qualitative estimates are sufficient, then the displacement can be taken Gaussian in a certain class of input parameters. However quantitative analysis doesn't cope with that approximation. It refers particularly to cases where statistics of large displacements should be investigated along with the theory of reliability. Anyway at least the

above approximate test should be used even if simple estimates are concerned. However, sophisticated tests being offered by mathematical statistics are recommended to be used.

4. Non-linear system of Duffing type with additive Poissonian excitation

The Duffing equation in a basic and in a normal form under an additive Poissonian excitation can be written as follows:

$$\begin{aligned} \ddot{x} + 2\,\omega_b\,\dot{x} - \omega_0^2 \cdot x\,(1 - \alpha^2\,x^2) = c \cdot Y(t) \quad \Rightarrow \\ \Rightarrow \quad \dot{x_1} = x_2\ , \\ \dot{x_2} = \omega_0^2\,x_1\,(1 - \alpha^2\,x_1^2) - 2\,\omega_b\,x_2 + c \cdot Y(t)\ . \end{aligned} \tag{15}$$

Drift and diffusion coefficients can be derived using formulae (3):

$$\kappa_1 = x_2\ , \qquad \kappa_2 = \omega_0^2\,x_1\,(1 - \alpha^2\,x_1^2) - 2\,\omega_b\,x_2\ , \tag{16}$$

Eqs (15), (16) enable to write down the GFP equation:

$$\begin{aligned} \frac{\partial p(x_1, x_2, t)}{\partial t} = -\frac{\partial [x_2\,p(x_1, x_2, t)]}{\partial x_1} - \frac{\partial [(\omega_0^2\,x_1(1 - \alpha^2\,x_1^2) - 2\,\omega_b\,x_2)\,p(x_1, x_2, t)]}{\partial x_2} - \\ - \lambda\,p(x_1, x_2, t) + \lambda \int_{-\infty}^{\infty} p(x_1, x_2 - c \cdot \zeta, t)\,p_z(\zeta)\,\mathrm{d}\zeta \end{aligned} \tag{17}$$

Eq. (15) can give a true picture of the Mieses frame under Poissonian excitation. Stiffness linear part is negative and so the system shows an unstable stationary point in the origin (0,0). Positions of two stable stationary points are $S_i \equiv (x_1 = \pm 1/\alpha, x_2 = 0)$, $i = 1, 2$. The repulsivity ratio in the origin depends on a relation of linear/non-linear parts of stiffness and on the Poissonian chain intensity.

The domain division into finite elements and other conditions are analogous to the previous case: $\omega_0^2 = 1.0$, $\omega_b = 0.1$ and non-linearity ratio $\alpha^2 = 0.1$. As far as in the Duffing SDOF system the cubic stiffness part and the damping are positive, then under Poissonian excitation an existence of the steady-state solution of the GFP Eq. (7) can be presumed. Moreover extensive numerical analyses affirmed, that this solution is unique and independent from a position of the initial point $(x_{1,0}, x_{2,0})$. The results character is given predominantly by internal structure of impulse amplitudes. If impulses are always unidirectional whatever is the width of uniform distribution of impulse amplitudes, the response PDF in the steady-state $p_{st}(x, \dot{x})$ always concentrates around stationary point S_1 or S_2 according to the effective impulse direction. We reach this conclusion even if the opposite stationary point is selected as an initial system state.

Selected results of computation are exhibited for the response steady-state cases in Fig. 8. Results corresponding with following excitation parameters are plotted successively on four rows: 1st row $\lambda = 4$, $r = 6$ – Fig. 8 parts (1a)–(1c); 2nd row $\lambda = 6$, $r = 6$ – Fig. 8 parts (2a)–(2c); 3rd row $\lambda = 10$, $r = 1$ – Fig. 8 parts (3a)–(3c); 4th row – Fig. 8 parts (4a)–(4c); arrangement in every row: (a) contour diagram; (b) axonometric view; (c) vertical sections through exes $x, \dot{x}$. Columns (a) and (c) imply that the velocity PDF remains symmetric with respect to origin. Impulse amplitudes are positive. It is obvious

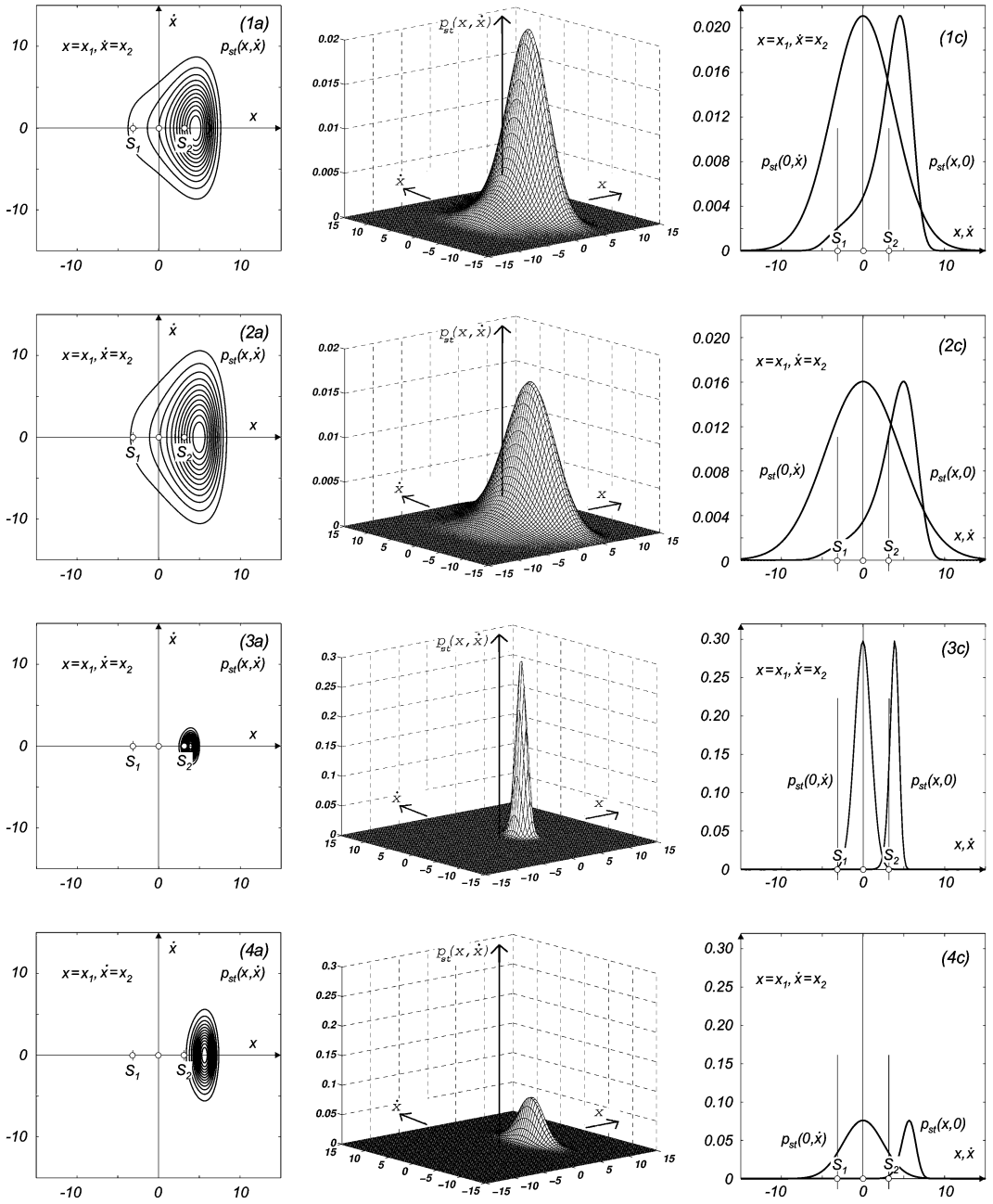

Fig.8: Response PDF of the Duffing system $\omega_0^2 = 1.0$, $\omega_b = 0.1$, $\alpha^2 = 0.1$ in a steady-state under Poissonian excitation; results are exhibited for four excitation parameters λ, r in individual rows; within every row : (a) contour diagram; (b) axonometric view; (c) vertical sections through the surface apex following axes x, $\dot{x}$

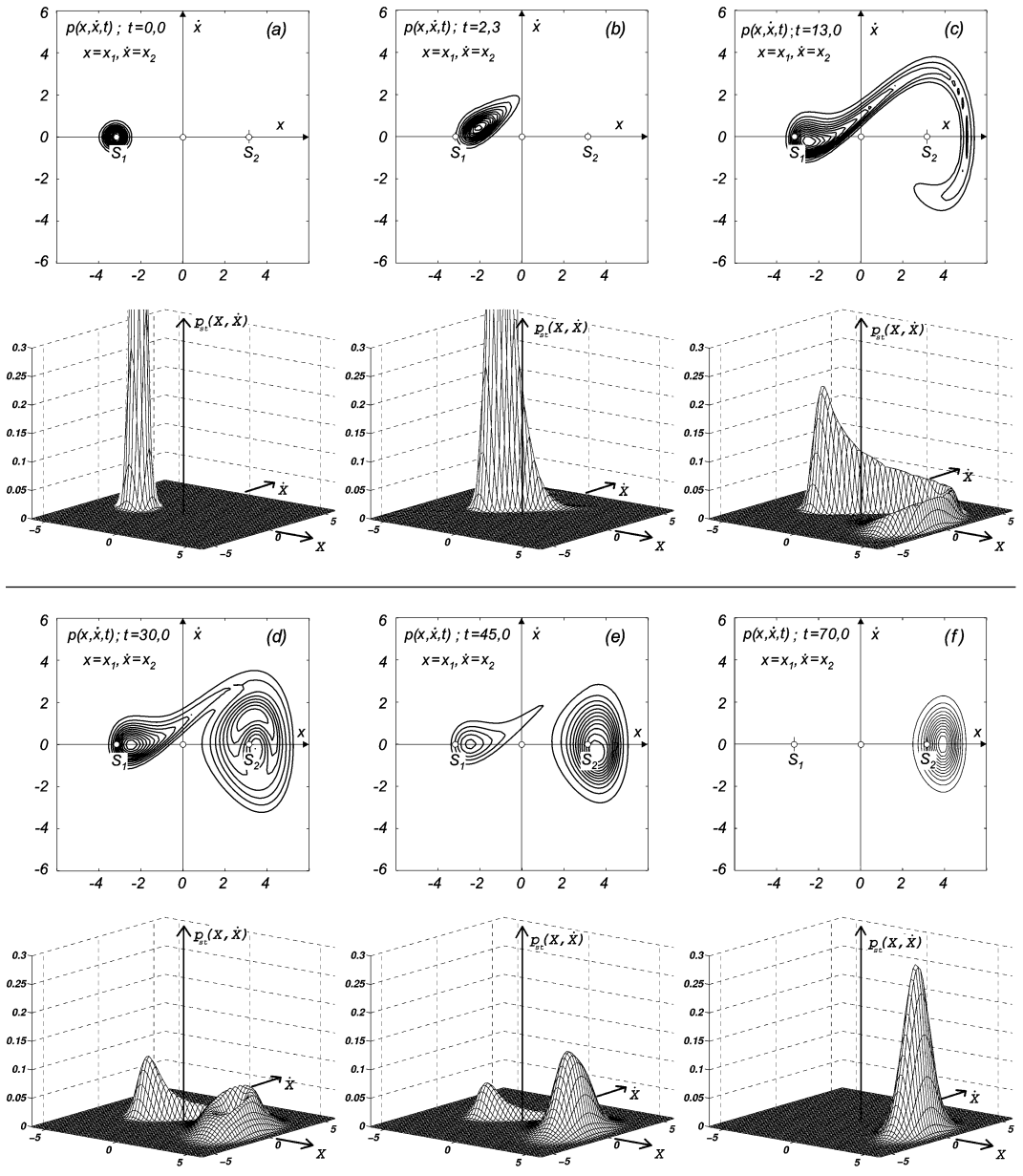

Fig.9: Time evolution of the response PDF of the Duffing system $\omega_0^2 = 1.0$, $\omega_b = 0.1$, $\alpha^2 = 0.1$, *excitation parameters* $\lambda = 10.0$, $r = 1$; *there are presented six shapes in the moments* $t = 0.0, 2.3, 13.0, 30.0, 45.0, 70.0$; *individual shapes are arranged in pairs (a)–(f), every pair consists of a contour diagram (upper picture) and axonometric view (lower picture)*

that the point S_2 affects as a concentrator of the displacement PDF, nevertheless a distinct deviation in the positive direction is visible. This type of deviation is general and it should be taken into account in applications. Under strong amplitudes $r = 6$ (1st and 2nd rows) the influence of the point S_1 is perceptible, as the PDF drop in S_1 neighborhood (the left part of the PDF) is visibly expressed. Nevertheless there didn't succeed to compose such structure of excitation and initial conditions that the result would have at least a slight bimodal character. Anyway we can conclude that the response PDF of the Duffing oscillator under Poissonian excitation has basically different character from those being produced by Gaussian white noise, see e.g. [8], [4].

The time evolution of PDF is not too interesting when starting at a positive impulse orientation from the initial condition (14) for the point S_2, or $(1/\alpha, 0)$. When moving with the initial condition from S_2 towards S_1, the transition process is getting more dramatic. An example is shown in Fig. 9, for the initial point $S_1 \equiv (-1/\alpha, 0)$. A series of individual snaps of the Duffing system response PDF evolution ($\lambda = 10.0$, $r = 1$ – 3rd row in Fig. 8) is drawn for six instances with approximately logarithmic distances: $t = 0.0, 2.3, 13.0, 30.0, 45.0, 70.0$. Each of these instances is characterized by one pair (a)–(f). Each pair consists of a contour diagram (upper picture) and of an axonometric view (lower picture). Starting the simulation process the PDF leaves the initial rotating shape of the initial condition (14). It gains a slightly elongated form and quickly decreases the hight. In the next phase the system breaks through the energetic barrier with important frequency and starts to 'flow around' the point S_2. The PDF starts later to concentrate to the vicinity of the point S_2, nevertheless in a small neighborhood of this point remains a certain concave area. However the S_1 point neighborhood is still important. In the last but one phase the PDF dominant part concentrates already around S_2. In the last period the PDF assumed the steady-state shape.

5. Conclusion

The study is a follow-up to earlier publications by authors of this paper. It relates to a number of references involved in FEM oriented numerical solution of either FP equation for Gaussian white noise or the GFP equation for additive Poissonian excitation. The GFP equation for the response PDF of a non-linear system remains linear just like the FP equation. It includes all difficulties similarly like the FP equation, as for instance a large number of space variables, exponentially increasing extent of the differential system for time evolution of PDF in nodes, etc.

Furthermore the GFP has an integro-differential character. This fact complicates an assembling of relevant finite elements. The reason of these troubles is a non-local character of the integro-differential operator of the convolution type. Whereas this problem has been bypassed in earlier papers using the Fourier transform in space coordinates, the authors decided to follow a direct way of FEM discretizaton. This approach eliminates the need of the inverse Fourier transform to the original. On the other hand there is necessary to work with unknowns with shifted variables where the processing of this shifting is ruled by the intensity and probability composition of the particular Poissonian excitation.

Numerical results demonstrate that the Poissonian additive excitation applied on linear systems leads to the PDF which can compared with the PDF of the Gaussian type, if a rough qualitative estimate of the result is satisfactory. When the quantitative analysis should be done it is necessary to realize the non-zero skewness of the resulting PDF and consequently

the non-symmetric character of displacement statistics. Also sharpness differs from the Gaussian one. These differences should be respect especially when small probabilities are analysed for high values of space coordinates. It is the case when dealing with the reliability problems, first excursion problems, etc.

Acknowledgement

The kind support of the Czech Science Foundation No. 103/09/0094, Grant Agency of the ASCR No. A200710805 and AV 0720710524 research plan are gratefully acknowledged.

References

[1] Lin Y.K., Cai G.Q.: Probabilistic Structural Dynamics – Advanced Theory and Applications, McGraw – Hill, New York, 1995
[2] Sniady P.: Dynamic response of linear structures to a random stream pulses, Journal of Sound and Vibration, 131 (1), 91–102, 1989
[3] Mironowicz W., Sniady P.: Vibration of linear structures due to jump-discontinuous, non-interrupted, stochastic processes, Earthquake engineering and structural dynamics, 19, 577–582, 1990
[4] Náprstek J., Král R.: Outline of numerical solution of the Fokker-Planck equation by means of the Finite Element Method, In: Proc. Dynamics of Machines 2008 (L. Pešek edt.), IT ASCR, Praha, 2008, pp. 77–86, 2008
[5] Bolotin V.V.: Random Vibrations of Elastic Systems (in Russian), Nauka, Moskva, 1979
[6] Pugachev V.S., Sinitsyn I.N.: Stochastic Differential Systems – Analysis and Filtering, J. Willey, Chichester, 1987
[7] Gihman I.I., Skorokhod A.V.: Stochastic Differential Equations, Springer, Berlin, 1972
[8] Wojtkiewicz S., Johnson E., Bergman L.A., Grigoriu M., Spencer B.F.: Response of stochastic dynamical systems driven by additive Gaussian and Poisson white noise: Solution of a forward generalized Kolmogorov equation by a spectral finite difference method, Computer Methods in Applied Mechanics and Engineering, 168, 73–89, 1999
[9] Arnold L.: Random Dynamical Systems, Springer, Berlin, 1998
[10] Náprstek J.: Some properties and applications of eigen functions of the Fokker-Planck operator, In: Proc. Engineering Mechanics 2005 (V. Fuis et al. eds), MT VUT Brno, Svratka, CD ROM, 12pp, 2005
[11] Di Paola M., Vasta M.: Stochastic integro-differential and differential equations of nonlinear systems excited by parametric poisson pulses, Int. Jour. Non-linear Mechanics, 8, 855–862, 1997
[12] Grigoriu M.: Response of dynamic systems to Poisson white noise, Journal of Sound and Vibration, 195, 375–389, 1996
[13] Grigoriu M.: A partial differential equation for the characteristic function of the response of non-linear systems to additive Poisson white noise, Journal of Sound and Vibration, 198 (2), 193–202, 1996
[14] Köylüoğlu H.U., Nielsen S.R.K., Iwankiewicz R.: Reliability of non-linear oscillators subject to Poisson driven impulses, Journal of Sound and Vibration, 176 (1), 19–33, 1994
[15] Köylüoğlu H.U., Nielsen, Cakmak A.S.: Fast cell-to-cell mapping (path integration) for non-linear white noise and Poisson driven systems, Structural Safety, 17, 151–165, 1998
[16] Tylikowski A., Marowski W.: Vibration of a non-linear single degree of freedom system due to Poissonian impulse excitation, Int. Journal Non-Linear Mechanics, 3, 229–238, 1986
[17] Vasta M.: Exact stationary solution for a class of non-linear systems driven by non-normal delta-correlated processes. Int. Jour. Non-linear Mechanics, 30, 407–418, 1995
[18] Grasman J., van Herwaarden O.A.: Asymptotic Methods for the Fokker-Planck Equation and the Exit Problem in Applications, Springer, Berlin, 1999
[19] Schueller G.I. (edt.): A state of the art report on computational stochastic mechanics, Probabilistic Engineering Mechanics – Special Issue, 12, 197–32, 1997

[20] Bergman L.A., Heinrich J.C.: Petrov-Galerkin finite element solution for the first passage probability and moments of first passage time of the randomly accelerated free particle, Computer Methods in Applied Mechanics and Engineering, 27, 345–362, 1981
[21] Bergman L.A., Spencer B.F.: Robust numerical solution of the transient Fokker-Planck equation for nonlinear dynamical systems, In: Proc. IUTAM Symposium Nonlinear Stochastic Mechanics (N. Bellomo, F. Casciati eds), University Turin, Springer-Verlag, Berlin-Heidelberg, pp. 49–60, 1992
[22] Spencer B.F., Bergman L.A.: On the numerical solution of the Fokker-Planck equation for nonlinear stochastic systems, Nonlinear Dynamics, 4, 357–372, 1993
[23] Bergman L.A., Spencer B.F., Wojtkiewicz S.F., Johnson E.A.: Robust numerical solution of the Fokker-Planck equation for second order dynamical system under parametric and external white noise excitation, In: Proc. Nonlinear Dynamics and Stochastic Mechanics (W. Langford, W. Kliemann, N. Sri Namachchivaya, eds), American Mathematical Society, pp. 23–27, (1996)
[24] Masud A., Bergman L.A.: Application of multi-scale finite element methods to the solution of the Fokker-Planck equation, Computer Methods in Applied Mechanics and Engineering, 194, 1513–1526, 2005
[25] Langley R.S.: A finite element method for the statistics of nonlinear random vibration, Jour. Sound Vibration, 101, 41–54, 1985
[26] Langtangen H.P.: A general numerical solution method for Fokker-Planck equations with applications to structural reliability, Probabilistic Engineering Mechanics, 6, 33–48, 1991
[27] Masud A., Khurram R.: A multiscale-stabilized finite element method for the advection-diffusion equation, Computer Methods in Applied Mechanics and Engineering, 193, 1997–2018, 2004
[28] Kloeden P.E., Platen E.: Numerical solution of Stochastic Differential Equations, Springer, Berlin, 1992
[29] Soize C.: Transient responses of dynamical systems with random uncertainties, Probabilistic Engineering Mechanics, 17, pp. 363–372, 2001

Received in editor's office: May 5, 2010
Approved for publishing: June 4, 2010

Note: This paper is an extended version of the contribution presented at the national colloquium with international participation *Dynamics of Machines 2010* in Prague.